NIH Public Access
Author Manuscript
J Neural Eng. Author manuscript; available in PMC 2009 May 8.

Published in final edited form as:
J Neural Eng. 2009 February ; 6(1): 014001. doi:10.1088/1741-2560/6/1/014001.

Neuron network activity scales exponentially with synapse density

G J Brewer[1,2], **M D Boehler**[2], **R A Pearson**[2], **A A DeMaris**[2], **A N Ide**[2], and **B C Wheeler**[3]

1 *Departments of Neurology, Pharmacology, Southern Illinois University School of Medicine, Springfield, IL 62794-9626, USA*

2 *Medical Microbiology, Immunology and Cell Biology, Southern Illinois University School of Medicine, Springfield, IL 62794-9626, USA*

3 *Bioengineering, University of Illinois Urbana-Champaign, Urbana, IL 61801, USA, E-mail: gbrewer@siumed.edu*

Abstract

Neuronal network output in the cortex as a function of synapse density during development has not been explicitly determined. Synaptic scaling in cortical brain networks seems to alter excitatory and inhibitory synaptic inputs to produce a representative rate of synaptic output. Here, we cultured rat hippocampal neurons over a three-week period to correlate synapse density with the increase in spontaneous spiking activity. We followed the network development as synapse formation and spike rate in two serum-free media optimized for either (a) neuron survival (Neurobasal/B27) or (b) spike rate (NbActiv4). We found that while synaptophysin synapse density increased linearly with development, spike rates increased exponentially in developing neuronal networks. Synaptic receptor components NR1, GluR1 and GABA-A also increase linearly but with more excitatory receptors than inhibitory. These results suggest that the brain's information processing capability gains more from increasing connectivity of the processing units than increasing processing units, much as Internet information flow increases much faster than the linear number of nodes and connections.

1. Introduction

In cortical brain networks, synaptic scaling appears to adjust the sum of synaptic inputs to produce a characteristic rate of synaptic output (Leslie *et al* 2001, Wilson *et al* 2007), especially important during a certain critical period of development (Hensch 2005). However, neither the developmental transition from no synapses to a number effective for the generation of action potentials nor the output of a neuronal network as a function of synapse density has been definitively determined. Here, we immunochemically measured the development of synaptic density in cultured hippocampal neurons over a three-week period in two serum-free media: Neurobasal/B27 that was optimized for neuron survival (Brewer *et al* 1993) and NbActiv4 (Brewer *et al* 2008) that was further optimized for a spike rate. In order to increase the contribution of synaptic development from that in the serum-free medium Neurobasal/B27, we optimized three additional components previously shown to promote synaptic development: creatine (Brewer and Wallimann 2000, Ducray *et al* 2007), estrogen (Kumar and Foster 2002, Brewer *et al* 2006) and cholesterol (Pfrieger and Barres 1997, Goritz *et al* 2005). Concentrations of these ingredients were optimized for the highest spontaneous spike rate in networks of hippocampal neurons cultured on multi-electrode arrays (MEAs) (Brewer

Correspondence to: G J Brewer.

NIH-PA Author Manuscript
NIH-PA Author Manuscript
NIH-PA Author Manuscript

NIH-PA Author Manuscript

NIH-PA Author Manuscript

NIH-PA Author Manuscript

et al 2008). The parent and optimized media were used as tools to follow the development of synapses over a three-week period of culture and to correlate the expected increase in synaptic density with the increase in spontaneous spike rates.

2. Methods

2.1. Multi-electrode arrays and analysis

The MEAs from Multichannel Systems (MCS, Reutlingen, Germany) consist of 59 TiN_3 electrodes with diameters of 30 μm and spacing of 200 μm. The spontaneous activity on the MEAs was measured using an MCS 1100× amplifier at 25 kHz sampling with a hardware filter of 8–3000 Hz at 37 °C under continuous flow of hydrated, sterile 5% CO_2, 9% O_2, balance N_2 (AGA, Springfield, IL). MCRack software was used to collect and analyze the data from 90 s of recording followed by a high-pass software filter of 200 Hz. Since most of the spikes were of the same height and shape for a given electrode, we have reported mostly single units of activity. It is possible that the increased activity could be an increase in the number of units contributing to the detected spikes. In addition, the 200 μm separation of electrodes together with demonstrated recording sensitivity within a 15 μm radius (Nam *et al* 2004) preclude detection of the same unit on more than one electrode. Nevertheless, some counting of multi-units on a single electrode is likely if more than one soma is located within 15 μm of the electrode. We did not perform spike sorting to clarify this possibility.

The nature of inhibitory signaling was probed by the addition of the GABA-A antagonist, bicuculline methiodide (10 μM final; Sigma-Aldrich) from a 1:1 dilution of the medium with a 2× concentrated drug in the medium. Burst analyses were conducted with PCLAMP software with a burst criterion of ≥3 spikes within 100 ms (Axon Instruments, Foster City, CA).

2.2. Neuron culture

E18 rat hippocampal cells were plated at 500 cells mm^{-2} on a poly-D-lysine-coated substrate in either Neurobasal™/B27™ (Brewer *et al* 1993) (Invitrogen, Carlsbad, CA) or NbActiv4™ (Brewer *et al* 2008) (BrainBits, Springfield, IL). Signals were recorded for 90 s at 25 kHz and spikes sorted at 5 standard deviations above the noise. Inactive electrodes or electrodes with a spike frequency less than 0.033 Hz were culled.

2.3. Immunocytology for synapses

Immunocytology was performed as previously described (Brewer *et al* 2008). Briefly, to resolve more individual synapses without jeopardizing costly electrode arrays, neurons were plated at 160 cells mm^{-2} on glass coverslips (Assistent, Carolina Biologicals, Burlington, NC) coated with poly-D-lysine (Brewer *et al* 1993). Cultures were fixed in methanol for 10 min at 4 °C to detect GABA and NR1 immunoreactive synapses. For synaptophysin and GluR1 (AMPA) immunoreactivity, cells were fixed for 30 min in 4% paraformaldehyde and 0.03% glutaraldehyde in PBS (Invitrogen). Non-specific sites were blocked and cells were permeabilized for 5 min in 5% normal goat serum and 0.5% Triton X-100 in PBS. Primary and secondary antibodies were diluted in 5% NGS and 0.05% TX-100 in PBS. Cells were incubated overnight with primary antibodies at 4 °C: mouse-anti-$GABA_{\alpha\beta}$ (1:50, Chemicon, Temecula, CA), rabbit-anti-NMDA-R1 (1:100, Sigma, St. Louis, MO), mouse-anti-synaptophysin (1:1000, Sigma S5768) and rabbit-anti-GluR1 (1:3000, Upstate Biotechnology, Charlottesville, VA). After rinsing, cells were incubated for 1 h at 22 °C with either Alexa-fluor 568-conjugated affiniPure goat anti-mouse IgG (1:2000, Molecular Probes, Eugene, OR) together with Alexa-fluor 488 affiniPure goat anti-rabbit IgG (1:50) or Alexa-fluor 568 goat anti-rabbit IgG (1:100) together with Alexa-fluor 488 goat anti-mouse (1:300). After rinsing, coverslips were mounted and imaged through an Olympus 60×/1.42 objective. Images were recorded at 12 bit depth with a Retiga Exi CCD camera (QImaging, Surrey, BC, Canada).

NIH-PA Author Manuscript

NIH-PA Author Manuscript

NIH-PA Author Manuscript

2.4. Image analysis

Image-Pro+ software was used in digital analyses and display of immunostains. The large range of intensities of fluorescent puncta was separated into three or four classes to better resolve more synapses than the previously described two classes (Brewer *et al* 2008). A high Gauss 5 × 5 deconvolution kernel filter was used for 1 pass at a strength of 10. A rectangular area of interest was chosen to encompass a representative group of fibers in a rectangular area of 356 μm^2 (48.2 × 7.4 μm^2) or an entire field of 16000 μm^2, as indicated. The same rectangle was positioned over a fiber-rich area in each of the 16 images for each medium and stain. Starting with the brightest objects on a day 21 image, an optimum threshold was determined that produced the highest count of objects in the indicated size range without merging together as larger objects (saved as class 1). The next brightest threshold class was optimized for maximum count and saved as class 2. The faintest (or next to faintest) class was similarly determined for class 3 (or 4). These threshold values were uniquely determined for each stain and applied to all images of a particular immunostain. Different stains produced different thresholds. Values reported are the sum of the objects in all classes. In the case of $GABA_A$ and NR1 staining, whole fields of 16000 μm^2 were also analyzed and fields culled to reduce sampling artifacts if they were outside 2 standard deviations of the mean. Other parameters were the same as Brewer *et al* (2008). Briefly, comparisons between media were stained at the same time. Puncta area and mean density were measured. Puncta area limits were set at 0.05–10 μm^2 for NR1, GABA and synaptophysin and at 0.02–10 μm^2 for GluR1 (field size for 60× objective is 0.016 mm^2, minimum area of 0.02 μm^2 = 4 pixels and a minimum area of 0.05 μm^2 = 10 pixels). To avoid double counting, the function of the holes was set to 0–0.5. To avoid counting long strings of unresolved objects, roundness was set at 0–3. The displayed images were pseudocolored using the merge function.

2.5. Statistics

Statistical analyses were performed by student's *t*-test or 2-factor ANOVA with culture medium a split-plot within days in culture. In these cases of ANOVA, the *p* value is reported for the probability that no difference exists between the two media. All graphs display means and S.E.

3. Results

The optimized NbActiv4 medium produced higher spike rates earlier in network development than the parent Neurobasal/B27 (figure 1). At 3 weeks of development, spike rates were four-fold higher in NbActiv4 than in Neurobasal/B27. The per cent active electrodes also increased with time to a higher level in NbActiv4 than in Neurobasal/B27.

The higher variability of spike rates in NbActiv4 at 3 weeks correlates with the higher number of active electrodes with both more values just above zero and some very high rates that were examined to be sure that they were not noisy electrodes. This non-Gaussian log–log distribution is characteristic of highly active networks (Boehler *et al* 2007).

The burst nature of network firing rapidly with longer periods of intervening silence has been recently addressed (Wagenaar *et al* 2006). In our system, the spike burst characteristics after 3 weeks of development were analyzed as initial spontaneous properties and after addition of 10 μM bicuculline, a GABA-Aβ antagonist to probe release from inhibition in the network (Barbin *et al* 1993) (table 1). Overall per cent spikes in bursts ranged from 88 to 96%. Initial network burst criteria that were higher in NbActiv4 include burst duration, spikes/burst, bursts min^{-1} and burst spikes min^{-1}. Spikes outside of bursts were similar in the two media. Addition of bicuculline caused most burst parameters to increase in either medium, but burst duration and spikes/burst were lower in NbActiv4 medium after bicuculline than before. Conversely,

NIH-PA Author Manuscript

NIH-PA Author Manuscript

NIH-PA Author Manuscript

non-bursting spikes were increased by bicuculline in Neurobasal/B27 medium. These results suggest that networks in Neurobasal/B27 are more inhibited than those in NbActiv4.

In separate cultures plated at a lower density of 160 cells mm^{-2} to obtain better synaptic resolution, we immunostained for the presynaptic protein synaptophysin and the postsynaptic AMPA receptor GluR1. Figure 2 shows both individual synaptophysin and GluR1puncta as well as an overlapping portion seen as yellow puncta after 1, 2 or 3 weeks of culture in either Neurobasal/B27 (figures 2(A), (C), (E)) or NbActiv4 (figures 2(B), (D), (F)). Over the three-week period, more synaptophysin puncta and a larger increase in GluR1 puncta were seen in cultures with NbActiv4. Figure 2 also shows how the three classes of bright objects in the image at 21 days in NbActiv4 are automatically analyzed for synaptophysin (2G) and as four classes for the more numerous GluR1 (2H). Digital analysis of these puncta indicates that synaptic density increased with time in culture, and to higher levels in NbActiv4 than in Neurobasal/B27 by 3 weeks (figures 2(I) and (J)). Note that the GluR1 counts per area was more than two times higher than the synaptophysin counts, probably because not all GluR1 puncta are in synapses.

Figure 3 shows similar development of NR1 NMDA receptor and $GABA_{A\beta}$ receptor puncta. While levels of both NR1 puncta are higher in NbActiv4 than in Neurobasal/B27 at 7 days over rectangular regions of fibers (figures 3(A) and (B)), by 14 days they are about the same (figures 3(C) and (D)). Figure 3(G) shows the digital analysis of NR1 puncta as four classes of deconvolved images for superior contrast. We measured puncta in a rectangle of 356 μm^2 over representative areas of fiber tracks, like those shown in figures 3(A)–(F). The analysis of fiber bundles in 16 independent images (figure 3(I)) showed that NR1 puncta develop earlier in NbActiv4 than in Neurobasal/B27, but after 21 days, the density of puncta was only 25% higher in NbActiv4. Further, the density in fibers increased linearly with development in NbActiv4, but seemed to increase less rapidly from 14 to 21 days in Neurobasal/B27, suggesting that local fiber density caused NR1 receptor density to reach a maximum earlier in this medium.

For the inhibitory $GABA_A$ receptor staining, figure 3(J) also shows a linear increase in GABA receptors with time of development for both neurons in NbActiv4 and in Neurobasal/B27. However, the GABA receptor puncta density in NbActiv4 was 40% higher than in Neurobasal/B27 at 21 days. The increase in GABA receptors with time of development for both excitatory and inhibitory receptors is an example of homeostatic scaling (Wierenga *et al* 2005).

We determined the efficacy of the developmental increase in synapses by correlating the increase in synaptic density with the increase in spike rates. Figure 4 shows a high correlation of spike rate with synaptophysin synapse count. For neuronal networks in Neurobasal/B27, the spike rate scaled as a power function of synapses with an exponent coefficient of 5.9. For networks cultured in NbActiv4, the exponent was 97% larger at 11.6. The higher exponent for neurons in NbActiv4 indicates a functional advantage for the optimized nutrients in faster development shown here and a possible contribution of faster axon and dendrite growth in NbActiv4 (Brewer *et al* 2008).

4. Discussion and conclusion

The exponential correlation of synapse density with the spike rate is interesting in terms of how synaptic input codes for information transfer. The relationship of synaptic puncta to spike rate might not be linear because of silent synapses (Nakiyama *et al* 2005), extrasynaptic receptor clusters (Hardingham *et al* 2002) and possibly higher branching in NbActiv4 (Brewer *et al* 2008). Certainly, many other factors such as ion channel densities and their control by kinases are integral to the process of transforming synaptic input into action potential

NIH-PA Author Manuscript

NIH-PA Author Manuscript

NIH-PA Author Manuscript

information, but we used synaptophysin synapse density as a marker for a necessary early component on the input side of information processing. Although our cultures were seeded at a low density to more easily resolve synapses in a plane, the synapse density achieved varied with developmental time and nutrients up to 6000 synapses/neuron at spike rates averaging 4 Hz. At the higher neuron density at which spike rates were measured, synapse density is certainly higher, but too difficult to measure by the techniques used here.

The increased spike rate seen here in NbActiv4 compared to Neurobasal/B27 could be produced by a number of factors in addition to synapse density measured here. A slightly higher density of astroglia in NbActiv4 to quickly remove excitatory glutamate engenders recovery from desensitization and promotes higher firing rates, including more spikes per burst of activity (Boehler *et al* 2007). The reported early increase in axon length in NbActiv4 (Brewer *et al* 2008) could also contribute to increased connections per soma. Both presynaptic and postsynaptic receptor phosphorylation regulate channel activity (Wang *et al* 2006). Finally, the balance between inhibitory and excitatory synaptic efficacy could modulate activity (Wierenga *et al* 2005). The greater increase in bursts following addition of the GABA-A inhibitor bicuculline in networks in Neurobasal/B27 than in NbActiv4 suggests that there are more inhibitory synapses in the Neurobasal/B27 networks' contribution to lower spike rates.

Since brain data transmitted as spikes scale at an exponential, or at least supralinear, function of synapse density, as shown here in two-dimensional networks, the mammalian brain in three dimensions and higher density is likely to scale information transfer at an even higher function of synapses. In the mammalian brain, synapses per neuron are estimated at 8000 in the mouse cortex, 18000 in the rat hippocampus and 50000 in the human cortex (14). The 6000 synapses per neuron that we achieved in our low density planar rat hippocampal cultures suggest a good approximation to the *in vivo* density. The supralinear increase in the spike rate with connectivity is highly suggestive of the notion that the brain's processing advantage comes not only from its high degree of connectivity but also from the even greater increase in information flow (spike rate) that is enabled by that connectivity. The Internet provides a metaphor for the scaling of information processing, as it is claimed that Internet information flow scales supralinearly with the number of connections, perhaps as the square (Metcalfe's law), exponentially or $n\log(n)$ (Briscoe *et al* 2006). Even though our brain is slow by computer standards, a clear processing advantage is evident by raising the 50000 connections/neuron to a higher power.

Acknowledgements

This work was supported in part by NIH NS52233.

References

Barbin G, Pollard H, Gaiarsa JL, Ben Ari Y. Involvement of GABAA receptors in the outgrowth of cultured hippocampal neurons. Neurosci Lett 1993;152:150–4. [PubMed: 8390627]

Boehler MD, Wheeler BC, Brewer GJ. Added astroglia promote greater synapse density and higher activity in neuronal network. Neuron Glia Biol 2007;3:127–40. [PubMed: 18345351]

Braitenberg, V.; Schuz, A. Cortex: Statistics and Geometry of Neuronal Connectivity. Vol. 2. Berlin: Springer; 2004. p. 19-35.

Brewer GJ, Boehler MD, Jones TT, Wheeler BC. NbActiv4 medium improvement to Neurobasal/B27 increases neuron synapse densities and network spike rates on multielectrode arrays. J Neurosci Methods 2008;170:181–7. [PubMed: 18308400]

Brewer GJ, Reichensperger JD, Brinton RD. Prevention of age-related dysregulation of calcium dynamics by estrogen in neurons. Neurobiol Aging 2006;27:306–17. [PubMed: 15961189]

Brewer GJ, Torricelli JR, Evege EK, Price PJ. Optimized survival of hippocampal neurons in B27-supplemented Neurobasal, a new serum-free medium combination. J Neurosci Res 1993;35:567–76. [PubMed: 8377226]

NIH-PA Author Manuscript

NIH-PA Author Manuscript

NIH-PA Author Manuscript

Brewer GJ, Wallimann TW. Protective effect of the energy precursor creatine against toxicity of glutamate and beta-amyloid in rat hippocampal neurons. J Neurochem 2000;74:1968–78. [PubMed: 10800940]

Briscoe, B.; Odlyzko, A.; Tilly, B. Metcalfe's law is wrong; IEEE Spectrum. 2006. p. 34-9.www.spectrum.ieee.org

Ducray AD, Schlappi JA, Qualls R, Andres RH, Seiler RW, Schlattner U, Wallimann T, Widmer HR. Creatine treatment promotes differentiation of GABA-ergic neuronal precursors in cultured fetal rat spinal cord. J Neurosci Res 2007;85:1863–75. [PubMed: 17526013]

Goritz C, Mauch DH, Pfrieger FW. Multiple mechanisms mediate cholesterol-induced synaptogenesis in a CNS neuron. Mol Cell Neurosci 2005;29:190–201. [PubMed: 15911344]

Hardingham GE, Fukunaga Y, Bading H. Extrasynaptic NMDARs oppose synaptic NMDARs by triggering CREB shut-off and cell death pathways. Nat Neurosci 2002;5:405–14. [PubMed: 11953750]

Hensch TK. Critical period plasticity in local cortical circuits. Nat Rev Neurosci 2005;6:877–88. [PubMed: 16261181]

Kumar A, Foster TC. 17beta-estradiol benzoate decreases the AHP amplitude in CA1 pyramidal neurons. J Neurophysiol 2002;88:621–6. [PubMed: 12163515]

Leslie, KR.; Nelson, SB.; Turrigiano, GG. Postsynaptic depolarization scales quantal amplitude in cortical pyramidal neurons; J Neurosci. 2001. p. 1-6.2008 Metcalfe's law http://en.wikipedia.org/wiki/Metcalfe%27s_law

Nakayama K, Kiyosue K, Taguchi T. Diminished neuronal activity increases neuron–neuron connectivity underlying silent synapse formation and the rapid conversion of silent to functional synapses. J Neurosci 2005;25:4040–51. [PubMed: 15843606]

Nam Y, Chang J, Khatami D, Brewer GJ, Wheeler BC. Patterning to enhance activity of cultured neuronal networks. IEEE Proc Nanobiotechnol 2004;151:109–15.

Pfrieger FW, Barres BA. Synaptic efficacy enhanced by glial cells in vitro. Science 1997;277:1684–7. [PubMed: 9287225]

Pinto, J. The 3 technology laws. 2002. http://www.jimpinto.com/writings/techlaws.html (Automation.com)

Wagenaar DA, Pine J, Potter SM. An extremely rich repertoire of bursting patterns during the development of cortical cultures. BMC Neurosci 2006;7:11–7. [PubMed: 16464257]

Wang JQ, Liu X, Zhang G, Parelkar NK, Arora A, Haines M, Fibuch EE, Mao L. Phosphorylation of glutamate receptors: a potential mechanism for the regulation of receptor function and psychostimulant action. J Neurosci Res 2006;84:1621–9. [PubMed: 16983660]

Wierenga CJ, Ibata K, Turrigiano GG. Postsynaptic expression of homeostatic plasticity at neocortical synapses. J Neurosci 2005;25:2895–905. [PubMed: 15772349]

Wilson NR, Ty MT, Ingber DE, Sur M, Liu G. Synaptic reorganization in scaled networks of controlled size. J Neurosci 2007;27:13581–9. [PubMed: 18077670]

NIH-PA Author Manuscript
NIH-PA Author Manuscript
NIH-PA Author Manuscript

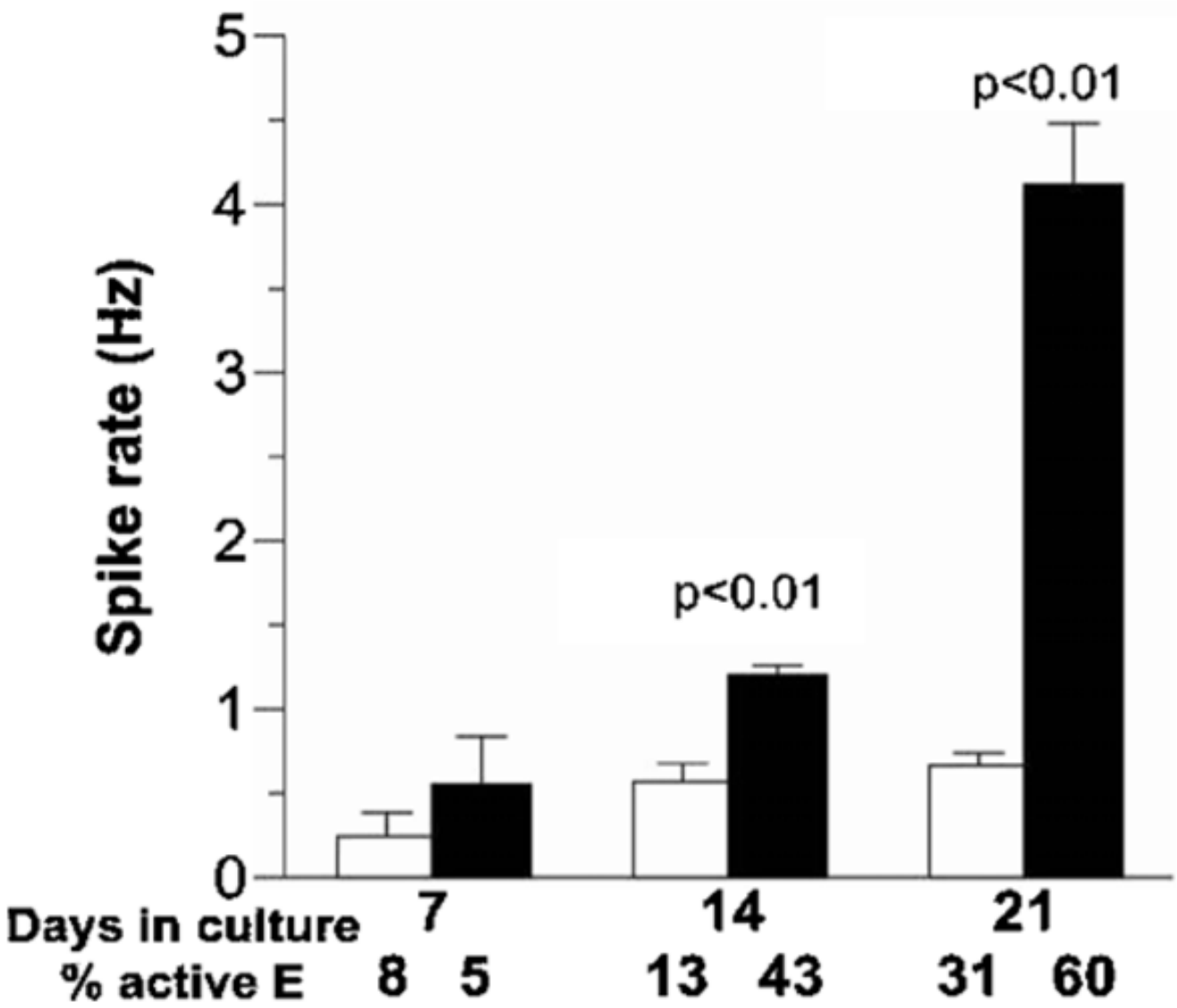

Figure 1.

Development of spontaneous action potentials in hippocampal cultures with NbActiv4 or Neurobasal/B27 media. Spontaneous activity over 0.03 Hz of neurons cultured in Neurobasal/B27 (open bars, $n = 3$ electrode arrays) or NbActiv4 (closed bars, $n = 3$) on multi-electrode arrays. Day 21 data are from an n of 5 electrode arrays each.

NIH-PA Author Manuscript
NIH-PA Author Manuscript
NIH-PA Author Manuscript

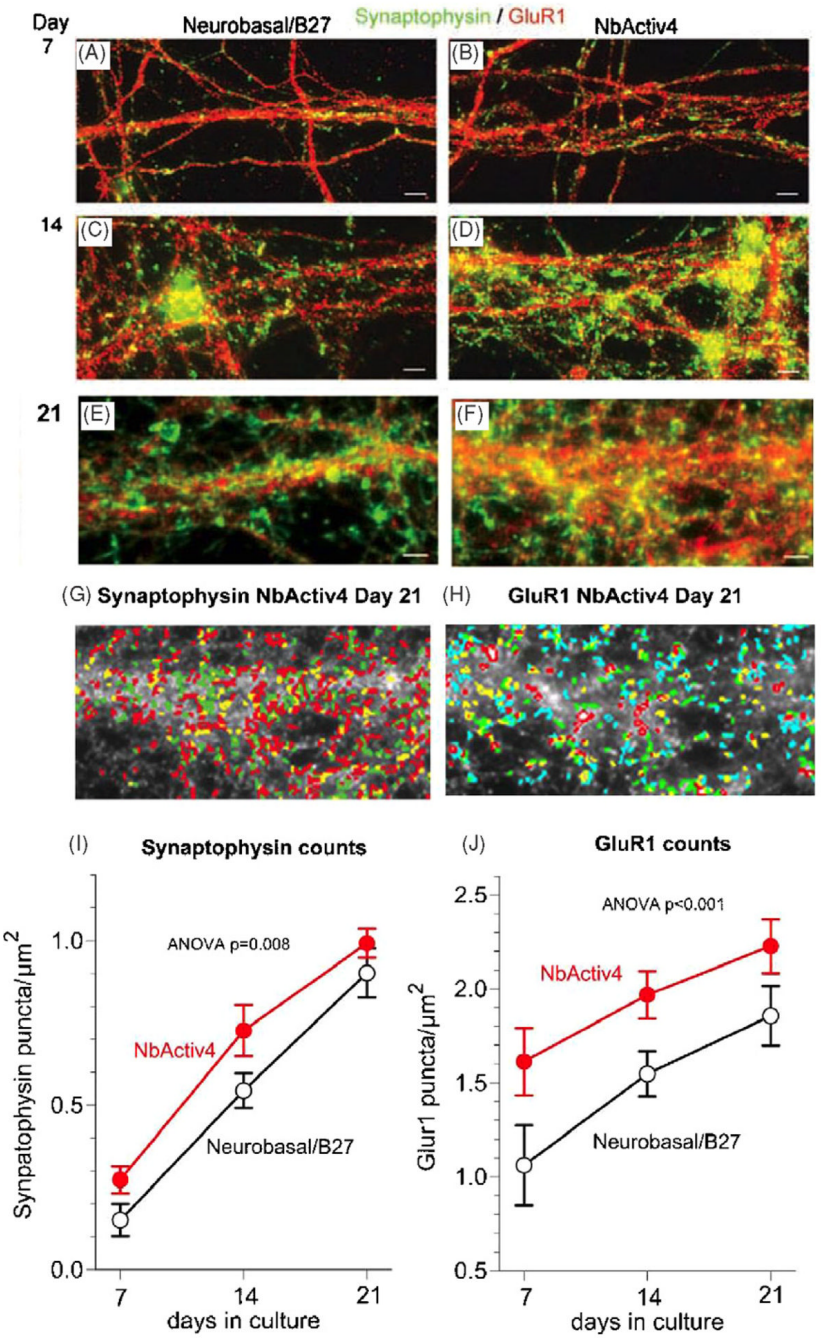

Figure 2.

Synaptic development of hippocampal neurons in NbActiv4 increases synaptophysin and GluR1 synaptic puncta earlier than in Neurobasal/B27. Green immunoreactive synaptophysin and red GluR1 puncta for neurons in Neurobasal/B27 ((A), (C) and (E)) or NbActiv4 ((B), (D) and (F)) cultured for 7 days ((A) and (B)), 14 days ((C) and (D)) or 21 days ((E) and (F)). Scale bars equal 20 μm. (G) Analysis of synaptophysin puncta by density separation into three classes from entire image in (F) (red—brightest, green, yellow—dimmest). (H) Similar analysis of GluR1 puncta by density separation into four classes (red—brightest, green, yellow, blue—dimmest). (I) Synaptophysin puncta densities for neurons increase linearly with development

in Neurobasal/B27 (black open symbols, $n = 16$) or NbActiv4 (red closed symbols, $n = 16$). (J) Similar linear increases for GluR1 puncta with time in culture.

NIH-PA Author Manuscript
NIH-PA Author Manuscript
NIH-PA Author Manuscript

NIH-PA Author Manuscript
NIH-PA Author Manuscript
NIH-PA Author Manuscript

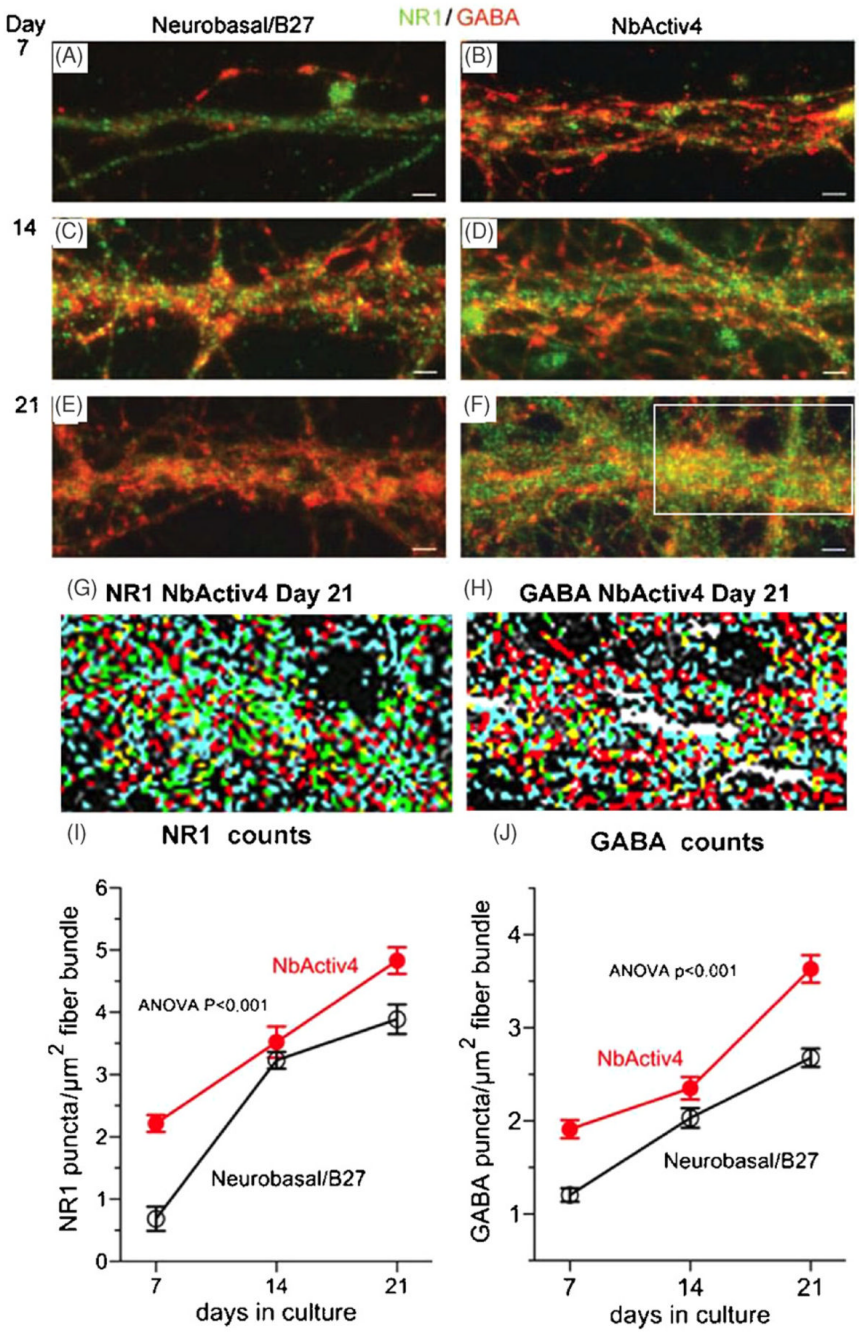

Figure 3.

Neurons in NbActiv4 increase development of NR1 and $GABA_A$ synaptic puncta faster than in Neurobasal/B27. Immunoreactive green NR1 and red GABA puncta in Neurobasal/B27 ((A), (C) and (E)) or NbActiv4 ((B), (D) and (F)) at day 7 ((A) and (B)), day 14 ((C) and (D)) or day 21 ((E) and (F)). Scale bars are 20 μm. Analysis of NR1 puncta (G) and GABA puncta (H) by density separation into four classes from region outlined in (F) (red—brightest, green, yellow, then blue—dimmest). (I) NR1 puncta densities increase linearly with development in Neurobasal/B27 (black open symbols, $n = 16$) or NbActiv4 (red closed symbols, $n = 16$). (J) Similar linear increases for GABA puncta with time in culture.

NIH-PA Author Manuscript

NIH-PA Author Manuscript

NIH-PA Author Manuscript

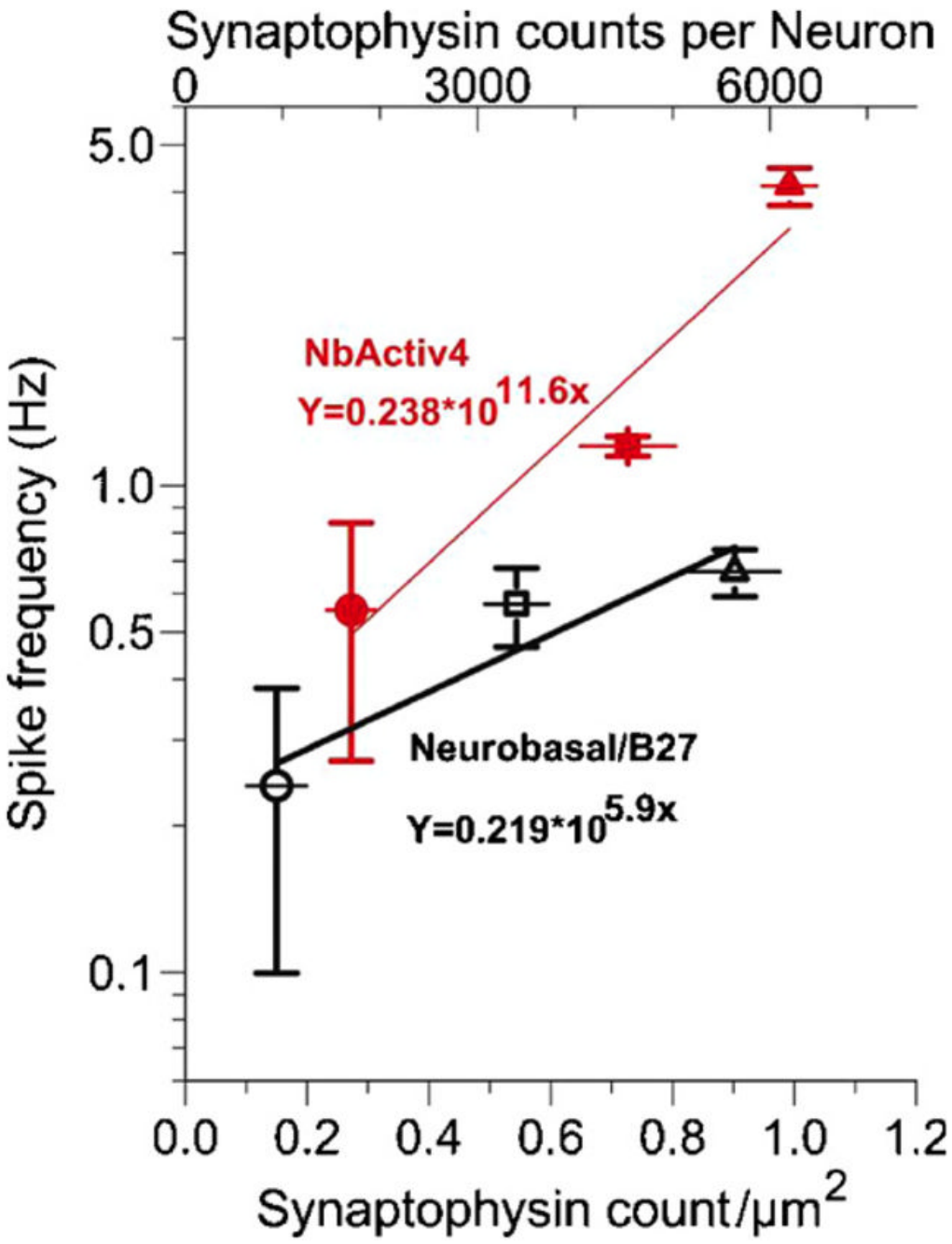

Figure 4.

Action potential frequency per synaptophysin density increases at an exponential rate. Spike frequency for neurons cultured in NbActiv4 (closed red symbols, $R^2 = 0.92$, $n = 3$) increases exponentially as a function of synapses 1.97 times that in Neurobasal/B27 (open black symbols, $R^2 = 0.88$, $n = 3$). The data are from figures 1 and 2 at developmental day 7 (circles), 14 (squares) and 21 (triangles).

NIH-PA Author Manuscript

NIH-PA Author Manuscript

NIH-PA Author Manuscript

Table 1

Analysis of burst behavior in 3 weeks[a].

	Initial		After bicuculline	
	Neurobasal/ B27, *n* = 32	**NbActiv4, *n* = 78**	**Neurobasal/B27, *n* = 47**	**NbActiv4, *n* = 70**
Duration of burst (ms)	133 ± 9	**245 ± 9.8**	**180 ± 27**	**137 ± 7**
		***p* < 10^{-4}**	***p*2 = 0.015**	***p*4 < 10^{-4}**
			***p*3 = 0.02**	
Intraburst interval (ms)	19.6 ±1.4	22.0 ± 0.7	**12.3 ± 1.1**	**17.2 ± 0.6**
		p not significant	***p*2 < 10^{-4}**	***p*4 < 10^{-4}**
			***p*3 < 10^{-4}**	
Spikes/burst	10.7 ± 1.0	**17.5 ± 0.9**	**23.4 ± 2.2**	**11.2 ± 0.7**
		***p* < 10^{-4}**	***p*2 < 10^{-4}**	***p*4 < 10^{-4}**
			***p*3 < 10^{-4}**	
Bursts min^{-1}	6.94 ± 0.90	**12.4 ± 0.8**	**10.3 ± 1.0**	**18.3 ± 1.2**
		***p* = 0.0001**	***p*2 = 0.018**	***p*4 = 0.0001**
			***p*3 < 10^{-4}**	
Burst spikes min−1	74.3 ± 17.3	**223 ± 26**	**240 ± 44**	178 ± 29
		***p* < 10^{-4}**	***p*2 = 0.0008**	*p*4 not significant
			*p*3 not significant	
Non-bursting spikes min^{-1}	10.4 ± 1.0	10.5 ± 1.3	**21.7 ± 4.8**	12.3 ± 2.6
		p not significant	***p*2 = 0.022**	*p*4 not significant
			*p*3 not significant	
% Burst spikes of total	88%	96%	92%	94%

[a] A burst is defined as ≥3 events within 100 ms detected by Clampfit's burst analysis tool. Bold indicates significant differences by *t*-test as compared below.

p = Initial condition comparison of Neurobasal to NbActiv4 media. *p*2 = Comparison in Neurobasal/B27 medium, before and after bicuculline. *p*3 = Comparison in NbActiv4 medium, before and after bicuculline. *p*4 = Comparison of Neurobasal to NbActiv4 media after bicuculline.